PHYSICAL REVIEW B **90**, 140101(R) (2014)

Correlation between electric-field-induced phase transition and piezoelectricity in lead zirconate titanate films

V. Kovacova,[1] N. Vaxelaire,[1] G. Le Rhun,[1] P. Gergaud,[1] T. Schmitz-Kempen,[2] and E. Defay[1,3,*]

[1]*CEA, LETI, MINATEC Campus, 17 rue des Martyrs, 38054 Grenoble Cedex 9, France*

[2]*aixACCT Systems GmbH, 52068 Aachen, Germany*

[3]*Centre de Recherche Public Gabriel Lippmann, Dept. Sci. & Anal. Mat, L-4422 Belvaux, Luxembourg*

(Received 27 June 2014; revised manuscript received 26 August 2014; published 6 October 2014)

We observed that electric field induces phase transition from tetragonal to rhombohedral in polycrystalline morphotropic lead zirconate titanate (PZT) films, as reported in 2011 for bulk PZT. Moreover, we evidenced that this field-induced phase transition is strongly correlated with PZT film piezoelectric properties, that is to say the larger the phase transition, the larger the longitudinal piezoelectric coefficient $d_{33,\mathrm{eff}}$. Although $d_{33,\mathrm{eff}}$ already reaches $130-150\,\mathrm{pm/V}$, our observation suggests that one could obtain larger $d_{33,\mathrm{eff}}$ values, namely $250\,\mathrm{pm/V}$, by optimizing the field-induced phase transition thanks to composition fine tuning as close as possible to the morphotropic phase boundary.

DOI: 10.1103/PhysRevB.90.140101 PACS number(s): 77.55.fg, 77.65.Bn, 77.80.B−

Although efficient lead-free piezoelectric thin films have been recently proposed in the literature [1–4], lead-based films as $Pb(Zr,Ti)O_3$ (PZT) [5,6] or $Pb(Mg,Nb)O_3-PbTiO_3$ ($PMN-PT$) [7] always exhibit the best piezoelectric properties. More specifically, they are strongly enhanced at the so-called morphotropic phase boundary (MPB) [8]. For PZT, the MPB is at the interface between the tetragonal and rhombohedral phases, while Zr/Ti atomic ratio is close to 52/48. In addition to these phases, the monoclinic phase might be present in the MPB, as evidenced in 1999 by Noheda *et al.* [9]. This phase coexistence and consequently the polarization mobility increase are thought to be the reason why piezoelectricity is enhanced in the MPB region. In 2011, Hinterstein *et al.* showed by *in situ* observations that bulk ceramic MPB PZT experiences structural changes while an electric field is applied [10]. More specifically, they reported that the application of an electric field reveals an increase of the monoclinic phase fraction. As they observed that most of PZT was composed of tetragonal and monoclinic phases, it strongly suggests that PZT experienced a tetragonal-to-monoclinic phase transition under electric field, and not only rotation of the polarization. An open question is therefore whether there is a correlation between large piezoelectric effects and this field-induced phase transition. Today it is widely believed that most of the piezoelectric effect is induced by domain wall switching. It is the so-called extrinsic contribution [11]. Several groups showed that PZT bulk and thin films in the tetragonal phase experience *a* to *c* domain switching while electric field is applied [12–15]. In this Rapid Communication we show that MPB PZT films experience *in situ* structural modifications versus electric field. We aim to correlate this field-induced phase transition with PZT films piezoelectric properties. This correlation could have a strong impact on piezoelectric material design for applications, as inkjet devices, integrated optical lenses, or microactuators in general [16].

In this study we prepared sol gel MPB PZT thin films. We characterized their piezoelectric coefficient $d_{33,\mathrm{eff}}$. X-ray diffraction (XRD) measurements were performed revealing PZT microstructure modifications when a dc-electric field was applied.

The substrates are 200 mm in diameter and made of Pt(111) $100\,\mathrm{nm}/TiO_2\ 20\,\mathrm{nm}/SiO_2\ 500\,\mathrm{nm}/Si\ 750\,\mu\mathrm{m}$. Thermal SiO_2 is grown at 1100 °C in oxygen. TiO_2 is obtained by depositing 10 nm of Ti followed by thermal annealing at 700 °C in oxygen for 30 min. Pt bottom electrode is sputtered at 450 °C. Each layer of PZT is spun, dried at 130 °C, and calcinated at 360 °C. The wafer is annealed at 700 °C for 1 min each time six layers have been deposited. This step enables us to crystallize PZT in the desired perovskite structure. Each single crystallized PZT layer is 60 nm thick. Eventually PZT thin film is 1 μm thick. As proposed by Calame *et al.* [5], the built-in composition gradient appearing in PZT sol gel can be dramatically decreased by using successive precursors with different compositions in order to decrease the composition variations. We have implemented this method with three different Zr/Ti ratio, namely 59/41, 52/48, and 43/57. Finally, the top electrode is made of 100 nm thick sputtered Ru. The designs realized in this study only involve Ru patterning to obtain the desired devices. Once resist has been deposited, exposed, and developed, Ru is wet etched with NaOCl. Finally, the resist is removed with acetone.

The piezoelectric coefficient $d_{33,\mathrm{eff}}$ has been measured with an AixACCT double-beam laser interferometry (DBLI) apparatus [17]. It requires polishing the substrate backside to insure a reflecting surface. The DBLI resolution is better than 1 pm/V. Therefore, the experimental accuracy is well below 1% as the measured deflections in this paper are in the nanometer range.

In order to achieve *in situ* XRD measurements, $7\times 7\,\mathrm{mm}^2$ samples with one $5\times 5\,\mathrm{mm}^2$ squared top electrode were prepared. Samples were then glued on a small piece of printed circuit board (PCB). Silver paste was spread on one cleaved side of the sample to contact the bottom electrode. 38 μm diameter gold wires were glued with silver paste between the sample electrodes and the PCB. Stronger isolated wires were then soldered between the PCB and the voltage supply.

$\theta/2\theta$ symmetrical measurements were performed on a D5000 Bruker diffractometer in a Bragg-Brentano configuration (BB). The *in operando* XRD measurements were

*defay@lippmann.lu

achieved with a four circle X-Pert Panalytical diffractometer using a polycapillary lens as primary optics and a crossed slit collimator with an aperture of $2 \times 2\,\mathrm{mm}^2$. Taking into account the beam divergence, the beam size on the sample is therefore about $3 \times 4\,\mathrm{mm}^2$. The secondary optic is a parallel plate collimator with a flat-graphite monochromator and a proportional detector. In both systems the x-ray source is a copper anode and a 1° offset has been applied in order to avoid the strong Si substrate reflections.

In order to define the samples' texture and phases present in PZT, pole figure measurements on planes {100}, {110}, {111} together with $\theta/2\theta$ scans from 20° to 102° were performed. The voltage impact on PZT was subsequently studied. For each voltage applied, longer acquisition $\theta/2\theta$ symmetrical scans were run around $\{100\}_t/\{100\}_r/\{001\}_t$ and their upper reflections orders, namely $\{200\}_t/\{200\}_r/\{002\}_t$ and $\{400\}_t/\{400\}_r/\{004\}_t$. t and r stand, respectively, for tetragonal and rhombohedral. The 2θ step width and duration were respectively 0.02° and 2 s for {100} and {200} planes. The time per step for {400} planes was 4 s. The 2θ range was [20.3, 23.3]°, [43, 46]°, and [95, 101]° for the first, second, and fourth order of (100) reflection, respectively. The successive voltages applied to the sample were 20, 10, 0, −10, −20, −10, 0, 10, 20, and 30 V. Note that no prepoling has been performed prior to this experiment.

The PZT XRD profiles were analyzed using two crystallographic space groups, namely tetragonal $P4mm$ and rhombohedral $R3m$ as well as ruthenium hexagonal $P63/mmc$. MAUD software [18] has been used to fit the experimental results. Assuming (100) fiber texture for both $P4mm$ and $R3m$ structures, the model has enabled us to quantify the phase percentage and the texture of the tetragonal phase. The crystallographic models used in the simulation were "polynomial" for background modeling, "standard function" for $P4mm$ and $R3m$ texture, and "isotropic size strain" for crystallite size and microstrain.

Measured $d_{33,\mathrm{eff}}$ at several positions of the sample are all in between 120 and 130 pm/V. This value is in line with the best values obtained for gradient free PZT as reported in Calame's thesis [19].

The BB diffraction experiments are shown in Fig. 1. Perovskite is the only visible phase, without any trace of pyrochlore. Figures 1(a), 1(b), and 1(c) shows the pole figures for planes {100}, {110}, and {111}. As the microstructure varies in ψ angle and is independent of φ angle, it proves that PZT has a strong $(100)_{r/t}$ fiber texture with a mosaicity of 6°. Although not represented here, rocking curves under different voltages on {200} planes show that mosaicity remains constant with electric field. Because these films exhibit a strong $(100)_{r/t}$ fiber texture, the constant mosaicity induces that the subsequent BB analysis of planes $\{n00\}$ performed along the fiber axis at different electric fields enable us to observe the behavior of nearly all the crystallites at once.

Figure 2 shows the BB diffraction profiles around (400) peaks at different voltages. The position of the (400) peaks for $P4mm$ and $R3m$ phases are also reported after the Inorganic Crystal Structure Database (ICSD)—92059 for $P4mm$, 24562 for $R3m$. Only {400} reflections are exploited since {100} and {200} reflections are at too low Bragg angles to be distinctly resolved. Although one should expect three peaks in this range,

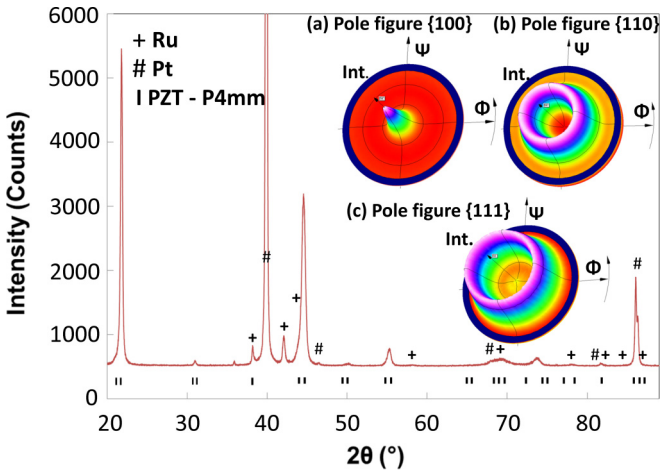

FIG. 1. (Color online) $\theta/2\theta$ profile and pole figures of PZT: (a) {100} pole figure, (b) {110} pole figure, and (c) {111} pole figure.

we only observe one experimental peak with contributions coming from $P4mm$ and $R3m$ phases as detailed later. This peak shifts towards lower angles when voltage is applied. The peak amplitude decreases with voltage. The amount of (004) $P4mm$ phase, that is to say tetragonal c domains, is invisible here and it does not change with voltage. Let us add the peaks position versus the applied voltage is reproducible, as will be shown in Fig. 4.

Figure 3 shows the peak profile refinement of the $\theta-2\theta$ scan achieved with MAUD in the vicinity of peaks $(400)_t$ and $(400)_r$ at 0 and 30 V. As already stated, only $P4mm$ and $R3m$ phases were identified in PZT. This is the same for all applied voltages as the peaks area is constant versus voltage, which means that no other phase appears with voltage. The Ru (202) peak is also shown in this area of interest. The $(004)_t$ signal is not visible whatever voltage is applied. Consequently, $P4mm$ c domains have not been considered in the refinement process. The Ru peak together with background have been fitted at 0 V and then kept constant for all other refinements. These limitations have not hindered a very satisfactory fit of all experimental data, as depicted in Fig. 3. At 0 V, $P4mm$ and $R3m$ phases are clearly identified. At 30 V, the amount of $R3m$ drastically increases and cancels out $P4mm$ occurrence. Note that there is no need to implement strain in the model to fit the experimental data.

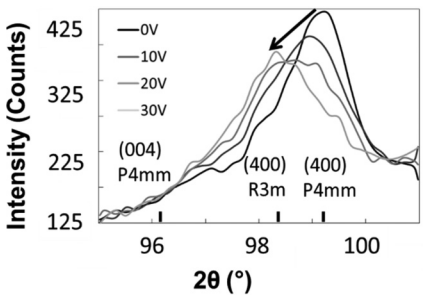

FIG. 2. $\theta-2\theta$ profile evolution of PZT around peak (400) vs different voltages. The positions of (400) peaks of $P4mm$ and $R3m$ phases are also indicated. The arrow underlines the peak behavior with voltage, namely low angle shift plus amplitude decrease.

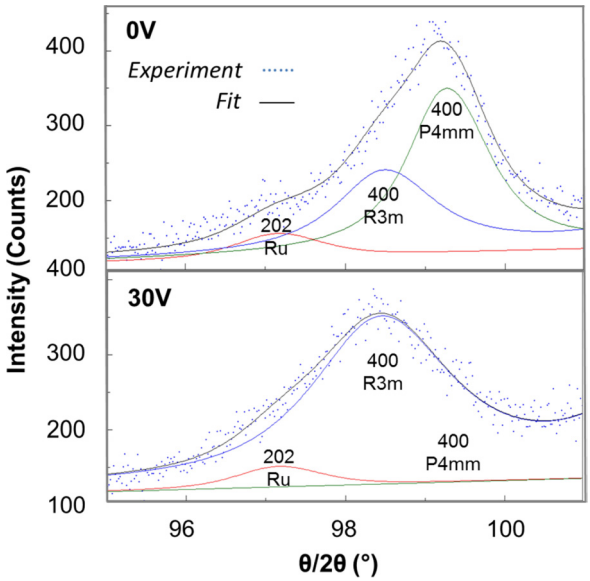

FIG. 3. (Color online) Refinement at 0 and 30 V of $\theta-2\theta$ scans of the PZT film. $(400)_r$, $(400)_t$, and Ru (202) reflection have been identified and fitted. The dots are experimental data, the black solid line corresponds to the sum of 202 Ru (red), 400 $R3m$ (blue), and 400 $P4mm$ (green) fits.

The relative volume proportion of phases $P4mm$ and $R3m$ versus voltage has been determined with MAUD and is shown in Fig. 4. Hence $R3m$ stands for 40% of the phase volume at 0 V and 100% at 30 V. This effect is approximately symmetrical when applying negative voltage. The experimental reproducibility has been used to assess error bars. It notably shows that there is no or very little hysteresis versus voltage.

As $P4mm$ and $R3m$ are the only phases, the increase of $R3m$ amount with voltage magnitude means that $P4mm$ volume decreases accordingly, that is to say there is a

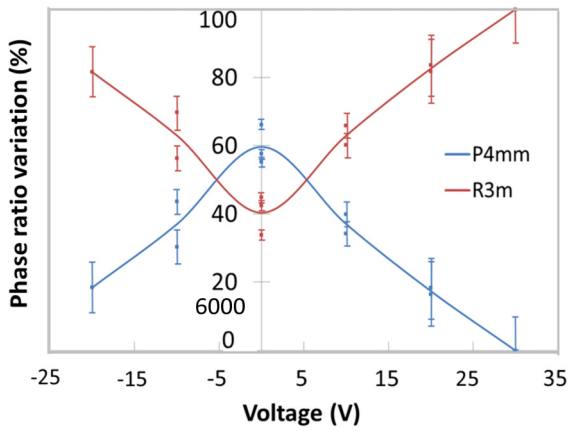

FIG. 4. (Color online) Phase variation versus applied voltage of PZT $P4mm$ and $R3m$ phases in the film. Solid points are the results of the profile refinement. There are two points for all voltages except at -20 and $+30$ V. Solid lines are guides for the eyes, based on the solid points' average value. Error bars are based on the reproducibility obtained at the same voltage.

voltage-induced phase transition. More specifically, as we observed that the appearance of tetragonal c domains is not visible, there is a phase transition from a oriented $P4mm$ to $R3m$. The transition between two phases of 52/48 PZT induced by electric field has already been reported by Hinterstein *et al.* [10] in bulk ceramic. They actually identified a transition from $P4mm$ to monoclinic Cm. In our study, $R3m$ fits better our results than Cm. Note that Cm is very similar to $R3m$, and has been stated as a rhombohedral-like phase by Hinterstein.

Besides, the fit gives the opportunity to roughly extract $d_{33,\mathrm{eff}}$ independently from the DBLI method. Indeed, we know (1) the amount of volume phase that has transited from $P4mm$ to $R3m$ (60% at 30 V) and (2) the peaks position (98.2° for $R3m$ and 99.2° for $P4mm$). This method gives $d_{33,\mathrm{eff}} = 150 \pm 25$ pm/V at 30 V, which is in the range of what has been measured with the DBLI method (120–130 pm/V). Therefore, it proves that the piezoelectric effect of this MPB gradient free PZT film is mostly due to the voltage-induced transition from tetragonal to rhombohedral phases. It is interesting to observe that, contrary to what is observed in tetragonal PZT, a to c domain switching is not visible in this experiment.

One can also compare this result with Landau-Ginzburg-Devonshire (LGD) theory prediction. Du *et al.* [8] deduced from LGD that the most favorable phase and orientation for single crystal/single domain PZT in order to maximize piezoelectricity is [100]-oriented rhombohedral in the MPB area. Here our result suggests that for polycrystalline [100]-oriented 52/48 PZT, it is better to work with PZT in the tetragonal phase, but still very close to the MPB in order to have the propensity to transit easily to the rhombohedral phase when the electric field is applied. We suggest that our result could enable us to improve even further $d_{33,\mathrm{eff}}$ by fine tuning PZT composition in order to exhibit 100% $P4mm$ phase at 0 V without losing the capability to induce its complete transition to 100% rhombohedral phase. The whole transition from 100% $P4mm$ to 100% $R3m$ should induce $d_{33,\mathrm{eff}}$ as high as 250 pm/V according to the peak positions method detailed in the previous section. That represents a 67% increase compared with our experimental $d_{33,\mathrm{eff}}$. Consequently, one should gently increase the amount of Ti into PZT in order for it to be slightly more tetragonal.

Finally, Fig. 2 suggests that one could obtain higher strain by using pure tetragonal PZT and transiting from 100% a domains to 100% c domains by applying voltage. However, Kobayashi *et al.* have recently observed that this complete a to c domains transition in pure tetragonal $PZT_{30/70}$ requires large electric field (0.4 MV/cm) and induces cracks into PZT [20]. This result suggests that only PZT compositions in an MPB zone provide sufficient polarization mobility to take advantage of phase transitions to enhance the piezoelectric properties.

In this Rapid Communication we observed by *in operando* x-ray diffraction that a tetragonal to rhombohedral phase transition is experienced by MPB 52/48 PZT thin films when an external electric field is applied. Moreover, the field-induced domain switching in the tetragonal phase appeared to be negligible in these films. Besides, the films' piezoelectric coefficient $d_{33,\mathrm{eff}}$ measured on the one hand with a piezoelectric setup and on the other hand deduced from x-ray peaks displacements versus the applied field appeared very similar.

This proves that there is a strong correlation between the piezoelectric properties and the field-induced phase transition in MPB PZT films. This result suggests that one could probably improve even further $d_{33,\mathrm{eff}}$ by favoring the field-induced phase transition notably by fine tuning PZT films composition.

The research described in this paper was supported by The French Ministry of Defense and the Direction Générale de l'Armement. The authors acknowledge access to the Nanocharacterization Platform (PFNC) at Minatec Campus in Grenoble (France).

[1] M. Pijolat, S. Loubriat, S. Queste, D. Mercier, A. Reinhardt, E. Defay, C. Deguet, L. Clavelier, H. Moriceau, M. Aid, and S. Ballandras, Appl. Phys. Lett. **95**, 182106 (2009).

[2] A. Kursumovic, E. Defay, O. J. Lee, C. F. Tsai, Z. X. Bi, H. Y. Wang, and J. L. MacManus-Driscoll, Adv. Funct. Mater. **23**, 5881 (2013).

[3] W. Liu and X. Ren, Phys. Rev. Lett. **103**, 257602 (2009).

[4] I. Fujii, S. Shimizu, K. Yamashita, K. Nakashima, N. Kumada, C. Moriyoshi, Y. Kuroiwa, Y. Fujikawa, D. Tanaka, M. Furukawa, and S. Wada, Appl. Phys. Lett. **99**, 202902 (2011).

[5] F. Calame and P. Muralt, Appl. Phys. Lett. **90**, 062907 (2007).

[6] J. Abergel, M. Allain, H. Michaud, M. Cueff, T. Ricart, C. Dieppedale, G. Le Rhun, D. Faralli, S. Fanget, and E. Defay, *IEEE International Ultrasonics Symposium, Dresden* (IEEE, Dresden, Germany, 2012), pp. 972–974.

[7] S. H. Baek, J. Park, D. M. Kim, V. A. Aksyuk, R. R. Das, S. D. Bu, D. A. Felker, J. Lettieri, V. Vaithyanathan, S. S. N. Bharadwaja, N. Bassiri-Gharb, Y. B. Chen, H. P. Sun, C. M. Folkman, H. W. Jang, D. J. Kreft, S. K. Streiffer, R. Ramesh, X. Q. Pan, S. Trolier-McKinstry, D. G. Schlom, M. S. Rzchowski, R. H. Blick, and C. B. Eom, Science **334**, 958 (2011).

[8] X. Du, J. Zheng, U. Belegundu, and K. Uchino, Appl. Phys. Lett. **72**, 2421 (1998).

[9] B. Noheda, D. E. Cox, G. Shirane, J. A. Gonzalo, L. E. Cross, and S. E. Park, Appl. Phys. Lett. **74**, 2059 (1999).

[10] M. Hinterstein, J. Rouquette, J. Haines, Ph. Papet, M. Knapp, J. Glaum, and H. Fuess, Phys. Rev. Lett. **107**, 077602 (2011).

[11] F. Xu, S. Trolier-McKinstry, W. Ren, B. Xu, Z.-L. Xie, and K. J. Hemker, J. Appl. Phys. **89**, 1336 (2001).

[12] D. Berlincourt and Helmut H. A. Krueger, J. Appl. Phys. **30**, 1804 (1959).

[13] M. Kohli, P. Muralt, and N. Setter, Appl. Phys. Lett. **72**, 3217 (1998).

[14] K. S. Lee, Y. K. Kim, S. Baik, J. Kim, and II Sub Jung, Appl. Phys. Lett. **79**, 2444 (2001).

[15] S. Osone, Y. Shimojo, K. Brinkman, T. Iijima, and K. Saito, Appl. Phys. Lett. **90**, 262905 (2007).

[16] P. Muralt, R. Polcawich, and S. Trolier-McKinstry, MRS Bull. **34**, 658 (2009).

[17] K. Prume, P. Muralt, F. Calame, T. Schmitz-Kempen, and S. Tiedke, J. Electroceram. **19**, 407 (2007).

[18] L. Lutterotti, S. Matthies and H. R. Wenk, International Union of Crystallography, Newsletter of the Commission for Powder Diffraction, **21**, 14 (1999).

[19] F. Calame, Ph.D. thesis, École polytechnique fédérale de Lausanne, 2007.

[20] T. Kobayashi, N. Makimoto, Y. Suzuki, H. Funakubo, T. Oikawa, A. Wada, and R. Maeda, Jpn. J. Appl. Phys. **52**, 09KA01 (2013).